

RESEARCH ARTICLE | JANUARY 19 2024

Development of visible light-responsive mono and co-doped TiO₂ for photocatalytic degradation of methyl orange dye

Z. Malik; S. A. Ibrahim ; A. R. Ainuddin; R. Hussin; Z. Kamdi

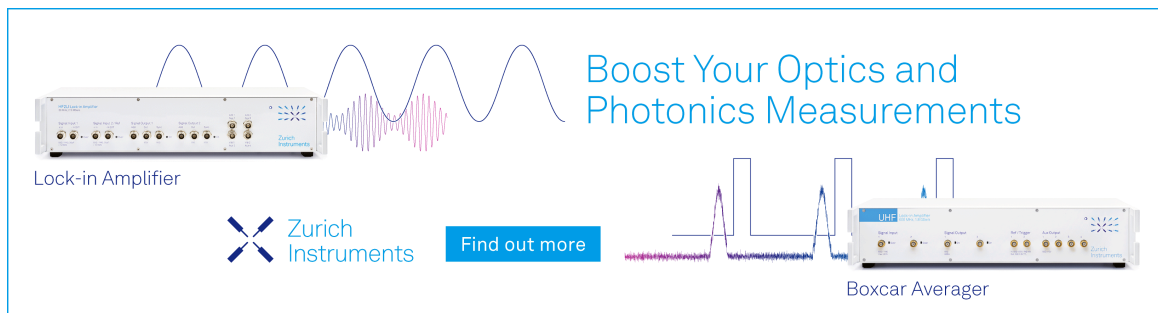


AIP Conf. Proc. 2925, 020058 (2024)

<https://doi.org/10.1063/5.0183197>




17 April 2024 03:18:31



Boost Your Optics and Photonics Measurements

Lock-in Amplifier

 Zurich Instruments

[Find out more](#)

Boxcar Averager

Development of Visible Light-Responsive Mono and Co-doped TiO₂ for Photocatalytic Degradation of Methyl Orange Dye

Z. Malik^{1, a)}, S.A. Ibrahim^{2, b)}, A.R. Ainuddin^{1, c)}, R. Hussin^{2, d)} and Z. Kamdi^{1, e)}

¹*Faculty of Mechanical & Manufacturing Engineering, Universiti Tun Hussein Onn Malaysia, Parit Raja, 86400 Batu Pahat, Johor Darul Takzim, Malaysia*

²*Faculty of Engineering Technology, Universiti Tun Hussein Onn Malaysia (Pagoh Campus), 84600 Panchor, Johor, Malaysia.*

^{a)} *myzaidimalik994@gmail.com*

^{b)} Corresponding author: *saida@uthm.edu.my*

^{c)} *ainun@uthm.edu.my*

^{d)} *rosniza@uthm.edu.my*

^{e)} *zakiah@uthm.edu.my*

Abstract. Titanium dioxide (TiO₂) has been acknowledged as a promising photocatalyst in environmental remediation including wastewater treatment. In this study, TiO₂ nanoparticles either by single or co-doped of iron (Fe) and nitrogen (N) via sol-gel method and calcined at 500 °C for 3 hours. This experiment investigated the performance of mono/co-dopant of TiO₂ photocatalyst against methyl orange in aqueous solution under UV light irradiation. The experimental results showed the rate of degradation favored in co-doped TiO₂ followed by mono doped TiO₂ and pristine TiO₂. The photocatalytic reaction followed pseudo first-order kinetics which were rationalized in terms of the Langmuir-Hinshelwood model and provided nearly complete degradation.

INTRODUCTION

Semiconductor-mediated photocatalytic oxidation can be utilised to eliminate organic contaminants from wastewater [1-3]. Among the semiconductors used, titanium dioxide (TiO₂) is known to be an excellent photocatalyst. TiO₂ has a high oxidation aptitude for dissolving organic compounds when exposed to UV light due to the existence of photogenerated holes in the valence band [4, 5]. The photocatalytic efficacy of such materials, together with their chemical stability, low toxicity, and low cost of precursors, make them potential candidates for ecologically friendly wastewater treatment methods. However, TiO₂ absorbs just a modest portion of the active solar spectrum, which accounts for approximately 5% of the solar light spectrum (UV light < 390 nm), limiting photocatalyst activity efficiency. Therefore, the development of visible-light responsive photocatalysts employing various techniques has received significant attention.

Many modifications have been made by various researchers to expand the photo-response of TiO₂ to the visible area. Method such as metal/nonmetal ion doping, surface dye sensitization and photosensitive material improvement are established [6-9]. Doping is a practical approach among all the modifications. Building active sites for the adsorption or catalysis of TiO₂ can be accomplished by adding heteroatoms like Iron (Fe) and Nitrogen (N). While N doping can provide a mid-gap state that acts as an electron donor or acceptor in the band gap, Fe³⁺ doping

can act as traps of the photogenerated electrons and holes and prevents electron-hole recombination [6, 10-12]. The reaction efficiency depends on the competition between the surface charge carrier transfer rate and the electron-hole recombination rate.

In this research, Fe and N-doped and co-doped TiO₂ were synthesized using the sol-gel method followed by calcination process at 500 °C for 3 h. The phase formation, morphology and photocatalytic activity behavior were investigated. In addition, the kinetic degradation of Methyl Orange (MO) was determined and presented in this study.

EXPERIMENTAL METHOD

All analytical-grade chemical reagents used for this process were from Aldrich or Merck and without additional purification. In this synthesis, the mono doped TiO₂ (Fe-TiO₂, N-TiO₂) and co-doped TiO₂ (Fe,N-TiO₂) followed the previous study by Teck et al [6] and Ibrahim et al [13], respectively.

Catalyst synthesis

Titanium isopropoxide (TTIP, C₁₂H₂₈O₄Ti) was used as a precursor for while ammonium nitrate (N₂H₄O₃) and iron nitrate (Fe(NO₃)₃·9H₂O) were employed as sources of dopant. Pure TiO₂ was synthesized by adding 20 ml TTIP was added drop wise into hydrolysis medium containing distilled water (7 ml), isopropanol (80 ml) and acetic acid (10 ml) under vigorous stirring at room temperature. The resultant transparent colloid suspension was stirred for 2 h and centrifuged at 3000 rpm for 20 min to obtain a precipitation. The formed precipitation was washed, dried overnight and calcined at 500 °C for 3 h. The same method was adopted for the synthesis of 10% (w/w) mono and co-doped TiO₂ (Fe-TiO₂, N-TiO₂ and Fe,N-TiO₂, respectively).

Characterization of catalysts

The characterization of the synthesized powders was investigated by X-Ray Diffraction (XRD), Field Emission-Scanning electron Microscope (FE-SEM) and Ultraviolet-Visible Spectrophotometer (UV-Vis). The XRD was performed using D8 Advanced Bruker System with Cu *ka* radiation in Rigaku diffractometer equipped with a rotating anode at 45 kV, over the range of 20°-80°. The Debye-Scherrer shown in Eq. 1 was used to calculate the crystallite size of samples.

$$D = \frac{K\lambda}{\beta} \cos \theta \quad (1)$$

where D is the crystal size of the catalyst, λ the X-ray wavelength (1.54 Å), β the full width at the half maximum (FWHM) of the catalyst, K a coefficient (0.89) and θ is the diffraction angle.

The morphology of the samples was observed by FESEM (JOEL, JSM-7600F). The UV-Vis absorption spectra were obtained using a UV-Vis spectrophotometer (Shimadzu, UV-1800).

Photocatalytic degradation

The photocatalytic activity was carried out by degrading MO with photocatalyst under visible light irradiation (400 W Flood Lamp, LED). A 0.05 g powdered photocatalyst (pure and doped TiO₂) was added into a beaker containing 50 ml of MO (10 ppm). The MO-catalyst solution was stirred for 30 mins in the dark to ensure equilibrium adsorption prior to photodegradation. At a given time interval of irradiation, 5 ml of the solution is withdrawn and centrifuged for measurement with UV-Vis spectrophotometer. The maximal absorption wavelength (λ_{max}) for MO, which have characteristic absorption peaks at 465 nm is used for determining the dye concentration in the aliquots. The photodegradation efficiency (PE) was calculated using the following equation:

$$PE (\%) = \frac{C_0 - C}{C_0} \times 100\% \quad (2)$$

where, C_0 is the initial concentration of MO solution and C is the concentration of MO solution after photocatalysis [14].

RESULTS AND DISCUSSION

XRD was used to identify the phase structure and crystallite size. Figure 1 shows the XRD pattern for different sample of pure TiO₂, Fe-TiO₂, N-TiO₂ and Fe, N-TiO₂ calcined at 500 °C. The anatase (101) phase diffraction peaks are clearly visible for all samples located at $2\theta = 25.35^\circ$. No peak for the rutile and brookite phases is found across all samples. Due to the very low dopant concentrations in these samples, no iron oxide peak could be seen in the XRD pattern. This suggests that the Ti⁴⁺ ions in these samples have been replaced by Fe³⁺ ions given that both ionic radius is similar in size, 0.75 Å and 0.69 Å respectively [15]. The crystallite sizes for all prepared samples were calculated by applying the Scherrer formula (Eq. 1) on the anatase (101) and summarized in Table 1.

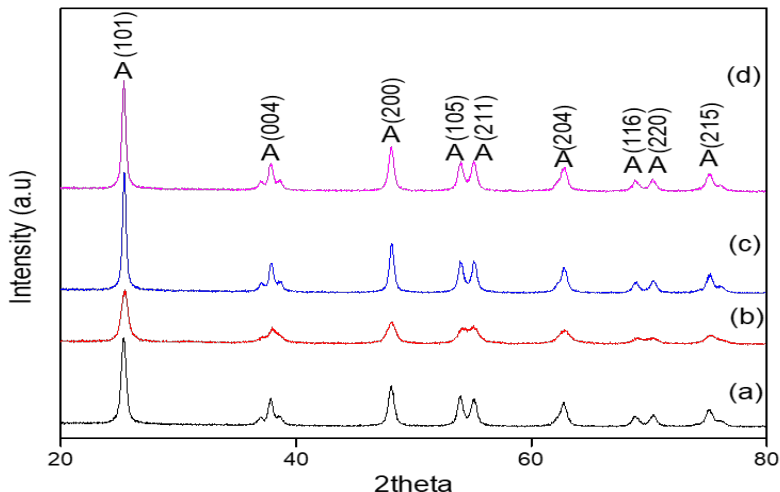


FIGURE 1. XRD pattern at 500 °C of (a) pure TiO₂, (b) Fe-TiO₂, (c) N-TiO₂ and (d) Fe, N-TiO₂ (A: Anatase)

TABLE 1. Crystallite size of the sample at different calcination temperature

Sample	Phase	Crystallite size (nm)
TiO ₂	Anatase	18.6
Fe-TiO ₂	Anatase	14.32
N-TiO ₂	Anatase	29.23
Fe, N-TiO ₂	Anatase	24.07

Figure 2 displays the FE-SEM images of 500 °C-calcined pure TiO₂, Fe-TiO₂, N-TiO₂, and Fe, N-TiO₂. All samples were seen to be agglomerated with uneven size and form, comparable to Teck and Ibrahim's findings [6]. The morphology of the samples appeared to be relatively rough, which could be advantageous in boosting the adsorption of reactants in various processes [16]

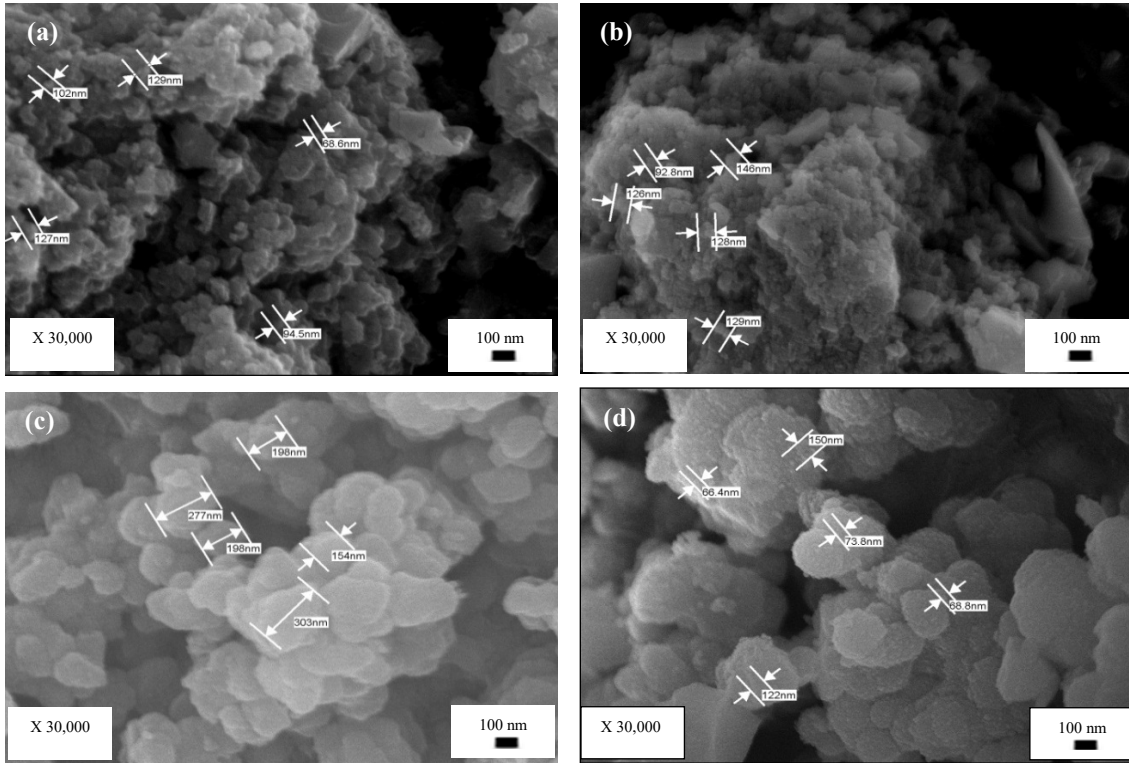


FIGURE 2. FE-SEM image of (a) pure TiO₂ (b) Fe-TiO₂ (300), (c) Fe, N-TiO₂ (500) and (d) Fe, N-TiO₂

The optical absorption spectra of the as-prepared samples were depicted in Figure 3. It is found that pure TiO₂ exhibited an onset of absorption edge at 400 nm determined by the intercept on the wavelength axis for a tangent drawn on absorption spectra. Compared with pure TiO₂, mono and co-doped TiO₂ shows a red shift of strong photo absorption in the visible region. The onset wavelengths were at 568 nm, 528 nm, 593 nm for Fe-TiO₂, N-TiO₂ and Fe, N-TiO₂, respectively. These indicates that mono and co-doped TiO₂ have highly potential for visible response of photoactivity.

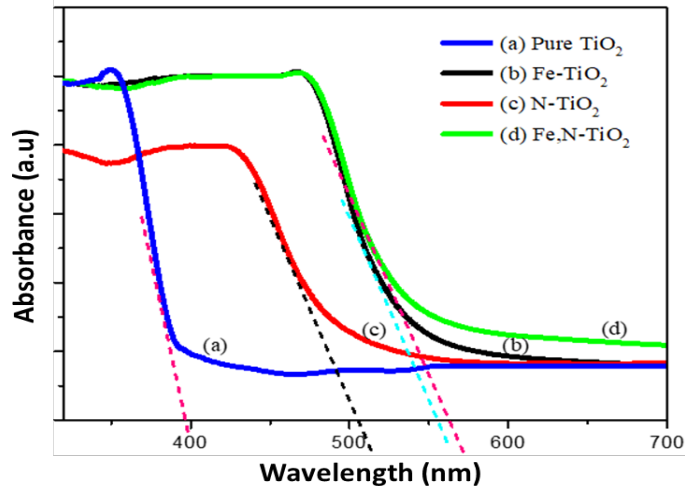


FIGURE 3. UV-Visible absorbance spectra

Figure 4(a) shows the photocatalytic activity of the as-prepared sample under visible light irradiation. The photocatalytic activities of the as-prepared catalysts indicate that pure TiO₂ showed very low activity for the degradation of MO compared to the others. The co-doped Fe,N-TiOs exhibited highest activities than those mono doped with N or Fe³⁺ alone. After 3 h of irradiation, the percentage removal of MO for pure TiO₂, Fe-TiO₂, N-TiO₂ and Fe, N-TiO₂ were 10.65 %, 88.26 %, 56.96 % and 96.46%, respectively. Meanwhile, the kinetic of MO degradation was determined using the following equation :

$$R = \frac{-dC}{dt} = k_r = \frac{k_r KC}{(1 + KC)} \quad (3)$$

where k_r is the reaction rate constant, K the adsorption coefficient of the reactant, and C the reactant concentration. When C is very small, the product KC is negligible with respect to unity. Setting the Eq. 3 at the initial conditions of the photocatalytic procedure, $t = 0$, the concentration transforms to $C = C_0$, which gives Eq. 4:

$$\ln \frac{C}{C_0} = k_{app} t \quad (4)$$

where k_{app} is the apparent first-order reaction constant. Kinetic parameters resulting from the application of Eq. 3 and percentage of MO degradation are summarized in Table 2. All reactions followed an apparent first-order kinetics model verified by the linear plots as shown in Figure 4 (b).

Based on these results, it is proven that the enhanced photocatalytic activity under visible light irradiation is related to optical absorption of the as-prepared samples as depicted in Figure 3. According to several studies, the band gap of TiO₂ may be reduced and visible light could be absorbed by adding new energy levels of transition metal ions (Fe³⁺/Fe⁴⁺) to the material by doping it with metal ions [17, 18]. Hu et al [19] suggested that co-doping of Fe³⁺ and N limited the recombination of the photogenerated electron and hole, with Fe³⁺ trapping the photogenerated electrons and N trapping the photogenerated holes, which increased photocatalytic activity. In a different work, Jia et al. [20] found that the co-doping of N and Fe affected the dipole moments and made it easier to separate the photogenerated electron-hole pairs by causing lattice deformation. As a result, the efficiency of photocatalysis would increase.

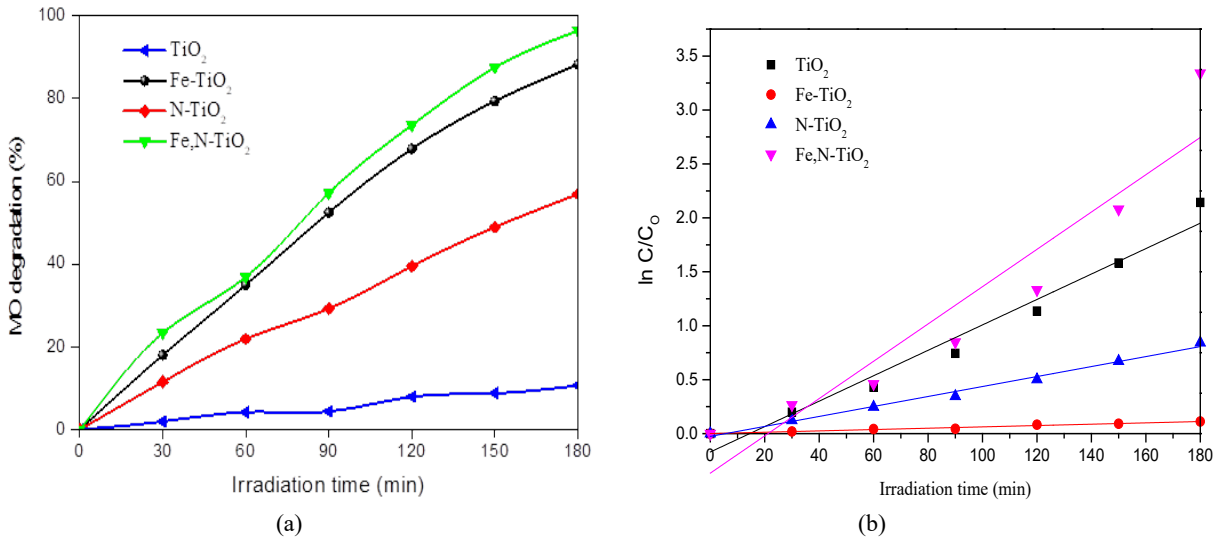


FIGURE 4 (a) Photocatalytic activities of the as-prepared photocatalyst in degrading MO under Visible light irradiation. (b) Plot of $\ln(C/C_0)$ vs irradiation time of different photocatalyst

TABLE 2. Kinetic analysis of the as-prepared sample under visible light irradiation

Sample	TiO ₂	Fe-TiO ₂	N-TiO ₂	Fe, N-TiO ₂
MO degradation (%) (After 3 h irradiation)	10.65	88.26	56.96	96.46
Degradation rate constant, k (x10 ⁻² min ⁻¹)	0.062	1.178	0.462	1.729
R ²	0.974	0.963	0.989	0.882

CONCLUSION

In this study, mono and co-doped TiO₂ using Fe and N as dopant were successfully synthesized via sol-gel method. The characteristic of the as-prepared sample and photocatalytic efficiency using MO degradation were investigated. The UV-Vis absorbance spectra shows that the mono and co-doped TiO₂ were red-shifted to visible region. The photocatalytic efficiency was enhanced from 10% to 96.46% as the introduction of Fe and N into TiO₂. The photocatalytic activity efficiency from the greatest to the lowest are as the following sequence: Fe, N-TiO₂ > Fe-TiO₂ > N-TiO₂ > TiO₂. The correlation between photocatalytic degradation and irradiation time demonstrated that the initial MO concentration was described by a pseudo-first-order model. As a conclusion, the visible response Fe, N- TiO₂ was deemed a promising technology for the degradation of organic pollutants in wastewater.

ACKNOWLEDGMENT

The authors would like to express their utmost gratitude and acknowledgement to the Universiti Tun Hussein Onn Malaysia for providing financial support for this project.

REFERENCES

1. J. Hong, K.-H. Cho, V. Presser, X. Su, *Current Opinion in Green and Sustainable Chemistry*, **36**, 100644 (2022).
2. M. Al Kausor, D. Chakraborty, *Inorganic Chemistry Communications*, **129**, 108630 (2021).
3. F.H. Azhar, Z. Harun, M.Z. Yunos, S.A. Ibrahim, R. Hussin, S.S. Alias, S.K. Hubadillah, T. Abdullahi, *Journal of Polymer Research*, **28**, 300 (2021).
4. D.S. Conceição, D.P. Ferreira, C.A.L. Graça, M.F. Júlio, L.M. Ilharco, A.C. Velosa, P.F. Santos, L.F. Vieira Ferreira, *Applied Surface Science*, **392**, 418-429 (2017).
5. A. Yamakata, J.J.M. Vequizo, *Journal of Photochemistry and Photobiology C: Photochemistry Reviews*, **40**, 234-243 (2019).
6. K.M. Teck, S.A. Ibrahim, *ARNP Journal of Engineering and Applied Sciences*, **11**, 8704-8709 (2016).
7. N.M. Arifin, F. Mohamad, R. Hussin, A.Z.M. Ismail, S.A. Ramli, N. Ahmad, N.H.M. Nor, M.Z. Sahdan, M.Z.M. Zain, M. Izaki, *Journal of Sol-Gel Science and Technology*, **100**, 224-231 (2021)
8. N. Sriharan, T.S. Senthil, P. Soundarajan, M. Kang, *Applied Surface Science*, **585**, 152719 (2022).
9. S.S. Alias, Z. Harun, F.H. Azhar, S.A. Ibrahim, B. Johar, *Journal of Cleaner Production*, **251**, 119448 (2020).
10. S.A. Ibrahim, M.K. Anwar, A.R. Ainuddin, A. Hariri, A.Z. M.Rus, Z. Kamdi, M.Z. Yunos, Z. Harun, *International Journal of Integrated Engineering*, **11**, 80-85 (2019).
11. X. Feng, L. Gu, N. Wang, Q. Pu, G. Liu, *Journal of Materials Science & Technology*, **135**, 54-64 (2023).
12. G. Divya, G. Jaishree, T. Siva Rao, M.L.V. Prasanna Chippada, K.V. Divya Lakshmi, S. Sai Supriya, *Hybrid Advances*, **1**, 100010 (2022).

13. S.A. Ibrahim, A.H. Zainal Alam, R. Hussin, Z. Kamdi, M.N. Mohamed Hatta, A.R. Ainuddin, M.Z. Yunos, [Journal of Science and Technology](#), **10**(2), 44-48 (2018).
14. Z. Malik, I.S. Aida, A. Ainun Rahmahwati, R. Hussin, K. Zakiah, [Key Engineering Materials](#), **908**, 406-413 (2022).
15. A.T. Kuvarega, R.W. Krause, B.B. Mamba, [Journal of Nanomaterials](#), **2014**, 962102 (2014).
16. C.M. Malengreaux, G.M.L. Léonard, S.L. Pirard, I. Cimieri, S.D. Lambert, J.R. Bartlett, B. Heinrichs, [Chemical Engineering Journal](#), **243**, 537-548 (2014).
17. M. Yang, C. Hume, S. Lee, Y.-H. Son, J.-K. Lee, [The Journal of Physical Chemistry C](#), **114**, 15292-15297 (2010).
18. W. Choi, A. Termin, M.R. Hoffmann, [The Journal of Physical Chemistry](#), **98**, 13669-13679 (1994)
19. S. Hu, F. Li, Z. Fan, C.-C. Chang, [Applied surface science](#), **258**, 182-188 (2011)